

Direct Inversion for the Squared Bessel Process and Applications

Simon J. A. Malham, Anke Wiese, and Yifan Xu

Maxwell Institute for Mathematical Sciences
and School of Mathematical and Computer Sciences
Heriot-Watt University, Edinburgh EH14 4AS, UK

December 24, 2024

Abstract

In this paper we derive a new direct inversion method to simulate squared Bessel processes. Since the transition probability of these processes can be represented by a non-central chi-square distribution, we construct an efficient and accurate algorithm to simulate non-central chi-square variables. In this method, the dimension of the squared Bessel process, equivalently the degrees of freedom of the chi-square distribution, is treated as a variable. We therefore use a two-dimensional Chebyshev expansion to approximate the inverse function of the central chi-square distribution with one variable being the degrees of freedom. The method is accurate and efficient for any value of degrees of freedom including the computationally challenging case of small values. One advantage of the method is that noncentral chi-square samples can be generated for a whole range of values of degrees of freedom using the same Chebyshev coefficients. The squared Bessel process is a building block for the well-known Cox-Ingersoll-Ross (CIR) processes, which can be generated from squared Bessel processes through time change and linear transformation. Our direct inversion method thus allows the efficient and accurate simulation of these processes, which are used as models in a wide variety of applications.

1 Introduction

The squared Bessel process is a one-dimensional diffusion process that plays a fundamental role in modelling economic and financial variables, see e.g., Göing-Jaeschke and Yor [9]. One important application is that it generates the well-known Cox-Ingersoll-Ross process, a mean-reverting square-root process that serves as a model in a wide variety of applications (see Vere-Jones and Ozaki [27] in seismology, Hu, Kessler, Rappel and Levine [10] in biology, and Cox,

Ingersoll and Ross [4] in finance). In this paper, we focus on its financial applications. The squared Bessel process also appears in describing key properties of Wiener processes, see for example Pitman and Yor ([20] and [21]), and Pitman and Winkel [19] for an overview. The correspondence between the squared Bessel process and square-root processes, or Cox-Ingersoll-Ross processes, is given by linear scaling and time change (see Jeanblanc, Yor, and Chesney [11], and Glasserman and Kim [8]). This simple correspondence means that results for squared Bessel process can be extended to square-root processes.

The transition probability of the squared Bessel process can be represented by a scaled non-central chi-square distribution, where the non-centrality parameter is given by what is known as the dimension of the squared Bessel process - the drift coefficient in the stochastic differential equation describing the process (see details in Sec 6.2 by Jeanblanc, Yor, and Chesney [11], and Revuz and Yor [23]). To simulate the squared Bessel process, we thus start with its transition probability density.

We propose a new direct inversion method to generate non-central chi-square samples, especially for the small degrees of freedom case, a computationally challenging situation that is relevant for financial applications, for example foreign exchange markets. Direct inversion was applied in Malham and Wiese [15], who derived a new direct inversion method to sample Generalized Gaussian random variables and showed that sums of powers of these generate chi-square samples. In our new direct inversion method, we use the direct inversion method to simulate the central chi-square samples directly. Importantly, we treat the degrees of freedom as a variable. Hence to simulate central chi-square variables, we establish a two-dimensional Chebyshev approximation with one of the variables being the degrees of freedom of the chi-square distribution. One of the advantages of the two-dimensional Chebyshev approximation is that a series of coefficients from the Chebyshev approximation is therefore valid for a whole range of values of the degrees of freedom. This flexibility in our method means that efficient and accurate pricing of options with different parameter values can be achieved. Gaß, Glau, Mahlstedt and Mair [6] applied a multi-dimensional Chebyshev method directly to approximate option prices. Acceptance-rejection methods to generate non-central chi-square samples were developed by Ahrens and Dieter [1], by Marsaglia and Tsang [17], and the generalized Marsaglia method by Malham and Wiese [15]. The reason we choose the direct inversion method instead of an acceptance-rejection method is that to generate the chi-square samples with small degrees of freedom, acceptance-rejection methods may reject a large number of samples, and this may be inefficient.

Section 2 provides the background to squared Bessel processes; we describe the relationship between the squared Bessel process and the Cox-Ingersoll-Ross process and the transition probability density of the squared Bessel process. In Section 3 we introduce our new direct inversion method to generate non-central chi-square samples, and we include a comparison of the relative errors in the first ten sample moments generated by our new method to other methods. In Section 4 we focus on the application of squared Bessel processes to the pricing of options. We illustrate the accuracy and efficiency of our new method in pricing path-independent put options on exchange rates, path-dependent Asian options and basket-options. We conclude in Section 5 and provide an outlook. The appendix contains the Chebyshev coefficients for a range of values of degrees of freedom.

2 The squared Bessel process and the CIR process

This section provides the background for the development of our direct inversion method and its application to the Cox-Ingersoll-Ross (CIR) process. We present the relationship between the squared Bessel process and the CIR process, and we derive the transition probability of the squared Bessel process through the transition probability of the Cox-Ingersoll-Roll process.

The squared Bessel process is the solution of the stochastic differential equation

$$dY_t = \delta dt + 2\sqrt{Y_t}dB_t,$$

where $Y_0 \geq 0$, and where $\delta \geq 0$ is a constant, and B is a Wiener process. For every initial value $Y_0 \geq 0$, a unique solution to the stochastic differential equation exists, see for example Jeanblanc, Yor and Chesney [11]. The parameter δ is known as the dimension of the squared Bessel process.

As introduced in Sec 6.3 by Jeanblanc, Yor, and Chesney [11], we define the function C as follows:

$$C(t) := \frac{c^2}{4b} (1 - e^{-bt}), \quad (1)$$

and set

$$X_t := e^{bt}Y_{C(t)},$$

where a , b , and c are positive constants satisfying $\delta = 4a/c^2$. Applying Itô's Lemma to X_t , we have

$$dX_t = (a + bX_t) dt + c\sqrt{X_t}dW_t, \quad (2)$$

where W is the Wiener process defined by $W_t := 2 \int_0^t (\sqrt{\exp(bs)}/c) dB_{C(s)}$.

We simulate the squared Bessel process by considering its transition probability density function following Malham and Wiese [15], who simulate the CIR process by using its transition probability density function. The transition probability of the squared Bessel process is shown in Theorem 2.1, quoted from Chapter XI in Revuz and Yor [23], who calculate this transition probability through the Laplace transform (for details see also Sec 6.2 in Jeanblanc, Yor, and Chesney [11]). Alternatively, the relationship between the squared Bessel process and the CIR process means that we can derive the transition probability density of the squared Bessel process through the known transition probability density of the CIR process.

Definition 2.1. *The distribution function $F_{\chi_\delta^2(\lambda)}$ for a non-central chi-square random variable is given for $y \in \mathbb{R}$ by*

$$F_{\chi_\delta^2(\lambda)}(y) = \frac{e^{-\lambda/2}}{2^{\delta/2}} \sum_{i=0}^{\infty} \frac{(\lambda/2)^i}{i!2^i\Gamma(\delta/2 + i)} \int_0^y x^{\delta/2+i-1} e^{-x/2} dx,$$

where δ is the degrees of freedom, λ is the non-centrality parameter, and $\Gamma(\cdot)$ is the standard gamma function.

Theorem 2.1. *Let Y be a squared Bessel process of dimension δ . Then for any $u_{n+1} > u_n$, given Y_{u_n} the conditional transition probability $P(Y_{u_{n+1}} < y | Y_{u_n})$ is given as $(u_{n+1} - u_n)$ times the non-central chi-square distribution with degrees of freedom δ and non-centrality parameter $\lambda := Y_{u_n}/(u_{n+1} - u_n)$, i.e., the conditional transition probability can be written as*

$$P(Y_{u_{n+1}} < y | Y_{u_n}) = F_{\chi_{\delta}^2(\lambda)}\left(\frac{y}{u_{n+1} - u_n}\right).$$

Proof. Consider a CIR process that satisfies the following SDE:

$$dX_t = (a + bX_t)dt + c\sqrt{X_t}dW_t, \quad (3)$$

where $a \geq 0$, $b \in \mathbb{R}$, and $c > 0$ are constants, and W is a Wiener process. We quote the transition probability of the CIR process from Cox et al. [4], Andersen[2] and Malham and Wiese [15]. Here we set $\delta := 4a/c^2$, and define the function $\eta(h)$ as follows:

$$\eta(h) := -4b \exp(bh)/c^2(1 - \exp(bh)),$$

where $h := t_{n+1} - t_n$ for $t_{n+1} > t_n$. Then we let $\lambda := X_{t_n} \eta(h)$. The transition probability of the CIR process from X_{t_n} to $X_{t_{n+1}}$ is

$$P(X_{t_{n+1}} < x | X_{t_n}) = F_{\chi_{\delta}^2(\lambda)}(x \cdot \eta(h) / \exp(bh)). \quad (4)$$

The relationship between the CIR process and the squared Bessel process in equation (2) states that $X_t = \exp(bt) \cdot Y_{C(t)}$. Using this transformation and the transition probability for X , the transition probability for Y is that as stated in the theorem. \square

To simulate the squared Bessel process from timestep u_n to u_{n+1} , we can generate a non-central chi-square sample with parameter $\lambda = Y_{u_n}/(u_{n+1} - u_n)$, then we have $Y_{u_{n+1}} = (u_{n+1} - u_n) \cdot \chi_{\delta}^2(\lambda)$.

3 Chi-square sampling

In order to design an efficient method to generate chi-square samples, we generate central chi-square samples first, and then use these to generate the non-central chi-square samples; see Malham and Wiese [15]. We propose a new direct inversion method to generate the central chi-square samples in this paper.

3.1 Central chi-square sampling

In our direct inversion method, a tensored two-dimensional Chebyshev polynomial expansion is used to approximate the inverse central chi-square distribution function $F_{\delta}^{-1}(u)$. To approximate

the inverse function accurately, we divide the range of $F_\delta^{-1}(u)$ into several regions based on the behaviour of the shape of its cumulative function. This is motivated by Moro [18] and Malham and Wiese [15] who split the range of the inverse function of the generalized Gaussian distribution into three regions based on the shape of the cumulative function to improve the approximation accuracy when using the direct inversion method to generate generalized Gaussian samples. Malham and Wiese [15] use inflection points to determine how to divide the domain. However, for the chi-square distribution there are no positive real roots of $F_\delta'''(w) = 0$ and $F_\delta''''(w) = 0$. Hence, we choose the two points w_- and w_+ to divide the domain of the cumulative function $F_\delta(w)$ into three regions by observing the behaviour of the chi-square cumulative function. In the first region, we have $w \in [0, w_-]$ or $u \in [0, F_\delta(w_-)]$, where the cumulative function shows a sharp increasing trend with a large slope. In the middle region, we have $w \in [w_-, w_+]$ or $u \in [F_\delta(w_-), F_\delta(w_+)]$, where the slope of the cumulative function decreases from a very large value to almost zero. In the tail region, we have $w \in [w_+, \infty)$ or $u \in [F_\delta(w_+), 1)$, where the cumulative function is flat and nearly equals one. To approximate the inverse central chi-square function $F_\delta^{-1}(w)$ in each region, we use a tensored two-dimensional Chebyshev polynomial expansion. One potential issue is that since the parameter δ is treated as one of the variables in the two-dimensional Chebyshev approximation, the boundary of each of the regions for the inverse variable u depends on the variable δ . This contrasts with the boundaries in a one-dimensional Chebyshev approximation. However, the regions for u are uniquely determined for each value of δ . We also divide the range of the variable δ , the degrees of freedom, in several intervals to achieve the accuracy as required. In what follows, we denote by $[c, d]$ such an interval for δ , where c and d are constants. We establish the two-dimensional Chebyshev approximation for each of the three regions of u .

Two-dimensional Chebyshev approximation. The inverse chi-square function $F_\delta^{-1}(u)$ can be approximated as follows:

$$F_\delta^{-1}(u) \approx \sum_{m=0}^M \sum_{n=0}^N c_{mn} T_m \left(\frac{2\delta - (d+c)}{d-c} \right) T_n(k_1 \xi(u) + k_2),$$

where T_m and T_n are, respectively, the degree m and n Chebyshev polynomials. Here ξ is a scaling function, specified below, that depends in the region for u . The linear transformation $2\delta - (d+c)/(d-c)$ in δ and k_1 and k_2 are chosen to map the regions for δ and for u to the interval $[-1, +1]$, on which the Chebyshev polynomials are defined. The values of M and N depend on the value of δ . A small value of δ will lead to large values of M and N . That means when the Chebyshev approximation is for chi-square samples with a small degree of freedom, more coefficients are needed to achieve the prescribed approximation accuracy. Motivated by Moro [18] and Malham and Wiese [16], we define the scaled and shifted variable $k_1 \xi(u) + k_2$ for each region as follows. The function $\xi(u)$ is defined as

$$\xi(u) = \begin{cases} u, & u \in [0, F_\delta(w_-)], \\ \log((1-u)\Gamma(\delta/2)), & u \in [F_\delta(w_-), F_\delta(w_+)], \\ \log(-\log((1-u)\Gamma(\delta/2))), & u \in [F_\delta(w_+), 1 - 10^{-8}]. \end{cases} \quad (5)$$

We choose $1 - 10^{-8}$ to be the upper boundary of the tail region. We label $\xi^{(1)}(u)$, $\xi^{(2)}(u)$, and $\xi^{(3)}(u)$ for $\xi(u)$ in the first, middle, and tail regions, and similarly for each of the three regions,

we also label $k_j^{(1)}$, $k_j^{(2)}$, and $k_j^{(3)}$ for each k_j , $j = 1, 2$. The values of $k_1^{(i)}$, and $k_2^{(i)}$ for $i = 1, 2, 3$ are chosen such that

- (i) $k_1^{(1)}\xi^{(1)}(0) + k_2^{(1)} = -1$, and $k_1^{(1)}\xi^{(1)}(F_\delta(w_-)) + k_2^{(1)} = 1$;
- (ii) $k_1^{(2)}\xi^{(2)}(F_\delta(w_-)) + k_2^{(2)} = -1$, and $k_1^{(2)}\xi^{(2)}(F_\delta(w_+)) + k_2^{(2)} = 1$;
- (iii) $k_1^{(3)}\xi^{(3)}(F_\delta(w_+)) + k_2^{(3)} = -1$, and $k_1^{(3)}\xi^{(3)}(F_\delta(1 - 10^{-8})) + k_2^{(3)} = 1$.

Coefficients of the two-dimensional Chebyshev expansion As in Trefethen [26] and Scheiber [24], the coefficients of the two-dimensional Chebyshev expansion can be calculated by the following formula:

$$c_{mn} = \begin{cases} \frac{1}{\pi^2} I_{mn}, & m = 0, n = 0, \\ \frac{2}{\pi^2} I_{mn}, & m = 1, n = 0, \\ \frac{2}{\pi^2} I_{mn}, & m = 0, n = 1, \\ \frac{4}{\pi^2} I_{mn}, & m \geq 1, n \geq 1, \end{cases}$$

with

$$I_{mn} = \int_{-1}^1 \int_{-1}^1 F^{-1}(\delta, u) \frac{T_m(\alpha)T_n(x)}{\sqrt{1-\alpha^2}\sqrt{1-x^2}} dx d\alpha,$$

where the inverse chi-square function is written as a two-variable function $F^{-1}(\delta, u) := F_\delta^{-1}(u)$. However, the inverse function $F^{-1}(\delta, u)$ is unknown. Therefore, to calculate the coefficients, the inverse function $F^{-1}(\delta, u)$ needs to be substituted when calculating the integral I_{mn} .

Let $x := k_1\xi(u) + k_2$. Based on the function $\xi(u)$ defined in equation (5), we have

- (i) $u = (x - k_2^{(1)})/k_1^{(1)}$ in the first region,
- (ii) $u = 1 - \exp\left(\left(x - k_2^{(2)}\right)/k_1^{(2)}\right)/\Gamma(\delta/2)$ in the middle region,
- (iii) $u = 1 - 1/\Gamma(\delta/2) \exp\left(\exp\left(\left(x - k_2^{(3)}\right)/k_1^{(3)}\right)\right)$ in the tail region.

For $\delta \in [c, d]$, let $\alpha := (2\delta - (d + c))/(d - c)$, so that $\delta = ((d - c)\alpha + (d + c))/2$, and define $\eta^{(i)}(x, \delta) := (x - k_2^{(i)})/k_1^{(i)}$ for $i = 1, 2, 3$. Let $I_{mn}^{(1)}$, $I_{mn}^{(2)}$, and $I_{mn}^{(3)}$ denote the integral I_{mn} of the coefficients c_{mn} in the three regions. We have the following expressions for the integral:

$$\begin{aligned} I_{mn}^{(1)} &= \int_{-1}^1 \int_{-1}^1 F^{-1}\left(\frac{(d-c)\alpha + (d+c)}{2}, \eta^{(1)}(x, \delta)\right) \cdot \frac{T_m(\alpha)T_n(x)}{\sqrt{1-\alpha^2}\sqrt{1-x^2}} dx d\alpha, \\ I_{mn}^{(2)} &= \int_{-1}^1 \int_{-1}^1 F^{-1}\left(\frac{(d-c)\alpha + (d+c)}{2}, 1 - \frac{\exp(\eta^{(2)}(x, \delta))}{\Gamma(\delta/2)}\right) \cdot \frac{T_m(\alpha)T_n(x)}{\sqrt{1-\alpha^2}\sqrt{1-x^2}} dx d\alpha, \\ I_{mn}^{(3)} &= \int_{-1}^1 \int_{-1}^1 F^{-1}\left(\frac{(d-c)\alpha + (d+c)}{2}, 1 - \frac{1}{\Gamma(\delta/2) \exp(\exp(\eta^{(3)}(x, \delta)))}\right) \cdot \frac{T_m(\alpha)T_n(x)}{\sqrt{1-\alpha^2}\sqrt{1-x^2}} dx d\alpha. \end{aligned}$$

Substituting u and δ for x and α yields

$$I_{mn}^{(i)} = \int_c^d G_\delta^{(i)}(u) \cdot \frac{T_m \left(\frac{2\delta - (d+c)}{d-c} \right)}{\sqrt{\delta(d+c) - \delta^2 - dc}} d\delta$$

for $i = 1, 2, 3$. The function $G_\delta^{(i)}(u)$ is defined as follows:

$$\begin{aligned} G_\delta^{(1)}(u) &:= \int_0^{F_\delta(w_-)} F^{-1}(\delta, u) \frac{T_n \left(k_1^{(1)} \xi(u) + k_2^{(1)} \right)}{\sqrt{1 - \left(k_1^{(1)} \xi(u) + k_2^{(1)} \right)^2}} du, \\ G_\delta^{(2)}(u) &:= \int_{F_\delta(w_-)}^{F_\delta(w_+)} F^{-1}(\delta, u) \cdot \frac{k_1^{(2)} \cdot T_n \left(k_1^{(2)} \xi(u) + k_2^{(2)} \right)}{(u-1) \cdot \xi(u) \cdot \sqrt{1 - \left(k_1^{(2)} \xi(u) + k_2^{(2)} \right)^2}} du, \\ G_\delta^{(3)}(u) &:= \int_{F_\delta(w_+)}^{1-10^{-8}} F^{-1}(\delta, u) \cdot \frac{k_1^{(3)} \cdot T_n \left(k_1^{(3)} \xi(u) + k_2^{(3)} \right)}{(1-u) \exp(\xi(u)) \sqrt{1 - \left(k_1^{(3)} \xi(u) + k_2^{(3)} \right)^2}} du, \end{aligned}$$

where $\xi(u)$ is defined in equation (5).

Let $w := F_\delta^{-1}(u)$, so that $F_\delta(w) = F_\delta(F_\delta^{-1}(u)) = u$, and $g_\delta^{(i)}(w) := G_\delta^{(i)}(F_\delta(w))$. Then we have

$$\begin{aligned} g_\delta^{(1)}(w) &= \int_0^{w_-} w \cdot \frac{T_n \left(k_1^{(1)} \xi(F_\delta(w)) + k_2^{(1)} \right) f_\delta(w)}{\sqrt{1 - \left(k_1^{(1)} \xi(F_\delta(w)) + k_2^{(1)} \right)^2}} dw, \\ g_\delta^{(2)}(w) &= \int_{w_-}^{w_+} w \cdot \frac{k_1^{(2)} \cdot T_n \left(k_1^{(2)} \xi(F_\delta(w)) + k_2^{(2)} \right) f_\delta(w)}{(F_\delta(w) - 1) \sqrt{1 - \left(k_1^{(2)} \xi(F_\delta(w)) + k_2^{(2)} \right)^2}} dw, \\ g_\delta^{(3)}(w) &= \int_{w_+}^{F_\delta^{-1}(1-10^{-8})} w \cdot \frac{k_1^{(3)} \cdot T_n \left(k_1^{(3)} \xi(F_\delta(w)) + k_2^{(3)} \right) f_\delta(w)}{(1 - F_\delta(w)) \exp(\xi(F_\delta(w))) \sqrt{1 - \left(k_1^{(3)} \xi(F_\delta(w)) + k_2^{(3)} \right)^2}} dw. \end{aligned}$$

However, the inverse value $F_\delta^{-1}(1 - 10^{-8})$ for the upper boundary of the integral above is unknown. We choose a large value, here we choose 20, such that $F_\delta(20) > 1 - 10^{-8}$, and use an indicator function to bound the inner function of the integral in the tail region as follows:

$$g_\delta^{(3)}(w) = \int_{w_+}^{20} \mathbb{I}_{(F_\delta(w) \leq 1-10^{-8})} \cdot w \cdot \frac{k_1^{(3)} \cdot T_n \left(k_1^{(3)} \xi(F_\delta(w)) + k_2^{(3)} \right) f_\delta(w)}{(1 - F_\delta(w)) \exp(\xi(F_\delta(w))) \sqrt{1 - \left(k_1^{(3)} \xi(F_\delta(w)) + k_2^{(3)} \right)^2}} dw.$$

The integrals are now transformed to a representation that is suitable for the calculation of the coefficients of the two-dimensional Chebyshev expansion in the three regions. These coefficients

in the three regions are calculated using Gauss-Konrod quadrature approximation using MATLAB with double precision. The calculation accuracy of the double integration of the coefficients is of order 10^{-8} .

Remark 1. The accuracy is influenced by the presence of singularities. When the chi-square variable w is close to the boundary of each region, or when the variable δ is close to the upper and lower boundaries c and d , the integrand tends to infinity, which decreases the accuracy in the calculation of the double integrals. The influence of w is greater than that of δ in the calculation of the double integral. To improve the accuracy, one potential way is to increase our double precision (16 digits) arithmetic to a larger digits arithmetic (for example 25 digits).

We have generated coefficients for different degrees of freedom by choosing different boundaries c and d for δ . In Table 1, we show the number of coefficients required in the three different regions to achieve $O(10^{-8})$ accuracy. Our direct inversion method achieves high accuracy approximation for any values of δ , especially for the challenging case of small values of δ . However, higher orders of Chebyshev polynomials are required for small δ . In the Appendix, we list the series of coefficients in the first region, middle region, and tail region for $\delta \in [0.1, 0.2]$.

Table 1: We show the orders of two-dimensional Chebyshev polynomials required to achieve $O(10^{-8})$ approximation accuracy. In each case, the pair shown is (M, N) , the orders of Chebyshev polynomials for the variables δ and u . The total number of Chebyshev coefficients in each region is $(M + 1) \times (N + 1)$.

δ	First region	Middle region	Tail region
[0.1, 0.2]	(5, 13)	(3, 11)	(3, 13)
[0.01, 0.02]	(4, 33)	(3, 13)	(3, 12)
[0.001, 0.002]	(4, 39)	(2, 13)	(3, 13)

Two-dimensional Clenshaw’s recurrence To generate central chi-square samples, we need to evaluate the sum of the two-dimensional Chebyshev series. We denote

$$S(x, y) = \sum_{m=0}^M \sum_{n=0}^N c_{mn} T_m(y) T_n(x)$$

the Chebyshev polynomial in our approximation for F_δ^{-1} . Recall x is the scaled variable of δ with $x = (2\delta - (d - c))/(d + c)$, and y is the scaled and shifted variable of u with different scaling as specified in equation (5) in the first region, the middle region and the tail region. A one-dimensional Chebyshev approximation can be evaluated efficiently using Clenshaw’s recurrence formula (see Sec 5.8 in Press et al [22]). As in Basu [3], to evaluate the two-dimensional Chebyshev series efficiently, we use Clenshaw’s recurrence for the variable y first and then again use the Clenshaw’s recurrence formula for the second variable x . The sum of all the terms of the Chebyshev series can be written as follows:

$$S(x, y) = \sum_{m=0}^M \sum_{n=0}^N c_{mn} T_m(y) T_n(x) = \sum_{n=0}^N a_n T_n(x),$$

where

$$a_n := \sum_{m=0}^M c_{mn} T_m(y).$$

The Chebyshev polynomials $T_m(y)$ and $T_n(x)$ have the recurrence relation as follows:

$$T_m(y) - 2yT_{m-1}(y) + T_{m-2}(y) = 0,$$

and

$$T_n(x) - 2xT_{n-1}(x) + T_{n-2}(x) = 0.$$

Define the quantities d_{mn} with $m = M, M-1, \dots, 1$ and $n = N, N-1, \dots, 1$ by the following recurrence:

$$\begin{aligned} d_{M+2,n} &= d_{M+1,n} = 0, \\ d_{mn} - 2yd_{m+1,n} + d_{m+2,n} &= c_{mn}. \end{aligned}$$

By solving the recurrence formula above we obtain the expression of d_{1n} and d_{2n} . Then we have

$$a_n = yd_{1n} - d_{2n} + c_{0n}.$$

Similarly, define the quantities g_n with $n = N, N-1, \dots, 1$ to solve the following recurrence:

$$\begin{aligned} g_{N+2} &= g_{N+1} = 0, \\ g_n - 2xg_{n+1} + g_{n+2} &= a_n. \end{aligned}$$

Solving this recurrence to obtain g_1 and g_2 , we then have the expression

$$S(x, y) = xg_1 - g_2 + a_0.$$

3.2 Non-central chi-square sampling

The method we use to generate the non-central chi-square samples using the central chi-square samples is taken from Malham and Wiese [15]. We describe this method briefly for completeness.

We distinguish two cases for the non-centrality parameter λ : the case $\lambda \leq 10$ and the case $\lambda > 10$. When $\lambda \leq 10$, then the non-central chi-square random variable $\chi_\delta^2(\lambda)$ is decomposed as $\chi_\delta^2(\lambda) \sim \chi_\delta^2 + \chi_{2N}^2$ (see Siegel [25], and Johnson [12]). Here χ_δ^2 can be generated by our direct inversion method proposed in the last section, and χ_{2N}^2 is a central chi-square random variable with degrees of freedom $2N$, where N is a Poisson distributed random variable with mean $\lambda/2$. We use the method in Glasserman [7] to generate χ_{2N}^2 . First we generate the Poisson distributed random variable N , and then we generate N independent uniform random variables U_1, \dots, U_N . Then $-2(\log(U_1) + \dots + \log(U_N))$ has a χ_{2N}^2 distribution, and

$$\chi_\delta^2(\lambda) \sim -2(\log(U_1) + \dots + \log(U_N)) + Z,$$

where Z is the χ_δ^2 random variable.

When $\lambda > 10$, the non-central chi-square random variable $\chi_\delta^2(\lambda)$ is decomposed as $\chi_\delta^2(\lambda) \sim \chi_{\delta+2N}^2 \sim \chi_{\delta+2\bar{N}+2P}^2$, using that N is a Poisson random variable, which can be expressed as a sum of two independent Poisson random variables \bar{N} and P with mean $10/2$ and mean $\lambda/2 - 10/2$, respectively. We generate a sample of the Poisson random variable \bar{N} , and consider the value of \bar{N} . If $\bar{N} \neq 0$, then we generate $\bar{N} - 1$ independent uniform random variables $U_1, \dots, U_{\bar{N}-1}$ and two independent standard normal random variables V_1 and V_2 . Then by the additivity property of non-central chi-square random variables, we have $\chi_\delta^2(\lambda) \sim -2(\log(U_1) + \dots + \log(U_{\bar{N}-1})) + V_1^2 + (V_2 + \sqrt{\lambda - 10})^2 + Z$, where Z is the χ_δ^2 random variable. When $\bar{N} = 0$, we set $\bar{\lambda} = \lambda - 10$. If $\bar{\lambda} > 10$, we repeat the process above, otherwise for $\bar{\lambda} \leq 10$ we use the algorithm of generating the non-central chi-square random variable with the non-centrality parameter smaller than 10 to generate the $\chi_\delta^2(\bar{\lambda})$ random variable.

3.3 Comparison

We illustrate the accuracy of our direct inversion method by considering the relative errors in the first ten sample moments of the simulated non-central chi-square samples. In Figure 1 these relative errors are displayed for three values of the degrees of freedom $\delta = 0.1, 0.01, 0.001$ (from top to bottom), and different values of the non-centrality parameter λ . The number of samples we use in each simulation is 5×10^7 . As can be seen in the six panels, the direct inversion method achieves consistently high accuracy among the different values of the degrees of freedom δ and non-centrality parameter λ . The relative errors are dominated by the Monte Carlo error. Comparing Figure 1 with Figure 4 in Malham and Wiese [15], where they show the relative errors in the first ten moments for the non-central chi-square samples simulated by three acceptance-rejection methods (Ahrens-Dieter [1], Marsaglia-Tsang [17], and Generalized Marsaglia [15]), the direct inversion method by Malham and Wiese [15], and the method by Andersen [2], we observe that our direct inversion method has the same high order of accuracy.

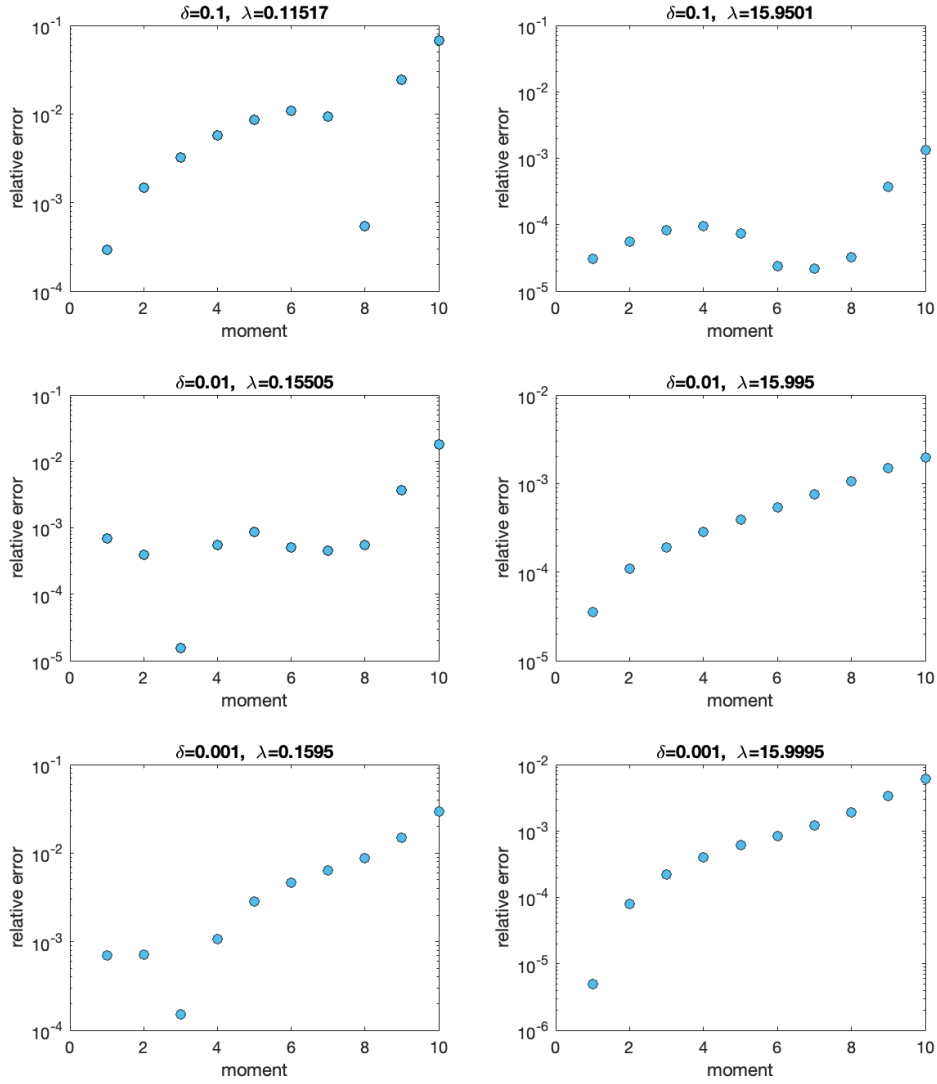


Figure 1: We show the relative errors in the first ten moments of the non-central chi-square samples using the direct inversion method. The simulations correspond to different values of degrees of freedom δ and non-centrality parameter λ . We test three values of degrees of freedom with $\delta = 0.1, 0.01, 0.001$, and the cases of $\lambda \leq 10$ and $\lambda > 10$ with values of $\lambda = 0.11517, 0.15505, 0.1595, 15.9501, 15.995, 15.9995$ (from top to bottom, and then from left to right). The number of samples in each case is 5×10^7 .

4 Applications

We apply our direct inversion method to the pricing of a standard European put option, an Asian option, and a basket option to show the efficiency of our method for path-independent, path-dependent and multi-asset options.

4.1 Path-independent options: a put option on an exchange rate

As an example of a path-independent option, we price a put option on an exchange rate that is modelled as a CIR process. First, we use our direct inversion method to simulate the squared Bessel process, which then generates the CIR process. The payoff of the put option is

$$\max(K - X_T, 0),$$

where K is the strike price, and X_T is the exchange rate at the expire time T . The price C_0 of the put option can be calculated as follows:

$$C_0 = \mathbb{E}[\max(K - X_T, 0)] = \int_0^K (K - x)f(x)dx,$$

where f is the probability density function. The CIR process X is given as in equation (3) by

$$dX_t = (a + bX_t)dt + c\sqrt{X_t}dW_t,$$

and its transition probability is shown in equation (4). Hence the density function can be calculated to be

$$f(x) = f_{\chi^2_{\delta}(\lambda)}(x \cdot \eta(h) / \exp(bh)) \cdot \eta(h) / \exp(bh),$$

where $f_{\chi^2_{\delta}(\lambda)}(z)$ is the density function of the non-central chi-square distribution. Therefore, the exact price of the put option can be calculated. Let \hat{X}_T denote the approximated asset price. Then \hat{C}_0 can be written as the expectation

$$\hat{C}_0 = \mathbb{E}[\max(K - \hat{X}_T, 0)].$$

The relative error of the approximation is defined as follows:

$$e := \frac{|C_0 - \hat{C}_0|}{C_0}.$$

We investigate the efficiency of our direct inversion method by considering the relative error, the CPU times, and the length of the timestep in the path simulation. As a comparison, we choose the full truncation Euler scheme by Lord, Koekoek and Dijk [13], and the quadratic-exponential scheme with martingale-correction by Anderson [2]. The full truncation Euler method is developed from the Euler method to avoid negative values when generating samples of the CIR process. The quadratic-exponential scheme with martingale-correction (QE-M) is an efficient

and robust method to generate samples of the CIR process for small values for the degrees of freedom (see details in Anderson [2]), consistent with our case.

Let Y be the squared Bessel process

$$dY_t = \delta dt + 2\sqrt{Y_t}dB_t,$$

with values $\delta = 0.18$, and $Y_0 = 0.09$. Then for the CIR process X given by

$$dX_t = a dt + bX_t dt + c\sqrt{X_t}dW_t$$

we set $a = 0.045$, $b = -0.5$, $c = 1$, so that $\delta = 4a/c^2 = 0.18$. Recall W is the Wiener process defined by $W_t = 2 \int_0^t (\sqrt{\exp(bs)}/c) dB_{C(s)}$, where $C(s) = (c^2/4b) \cdot (1 - \exp(-bs))$. The expiry time of the option is $T = 10$, the initial value of the asset is $X_0 = 0.09$, and the strike price is $K = 0.09$.

We use an equidistant partition of the time interval $[0, T]$ into N timesteps of length $h := T/N$. We show the relationship between the length h of the timesteps and the relative errors for the full truncation Euler method, the QE-M method, and direct inversion method, respectively, in Figure 2. The relative errors decrease with decreasing h for the full truncation Euler method and QE-M method. For the direct inversion method, there is no need to discretize, and only one timestep is needed to simulate one asset path if the option is path-independent. Hence for our direct inversion method, the relative errors are kept within the order of 10^{-3} for the different lengths of timesteps, showcasing the efficiency of this method for path-independent options.

In Table 2, we show the CPU times and the maximum length of the timesteps for each of the three methods in order to achieve at least order 10^{-3} accuracy in pricing the put option. As shown in Table 2, to achieve this accuracy, the direct inversion method is the most efficient in terms of CPU times. An important reason for this is the large number of timesteps used in the simulation of the CIR process in the full truncation Euler approximation to achieve the required accuracy. The length of timestep is $1/10$ for the full truncation Euler method, and $1/4$ for the QE-M scheme. However, as noted above our direct inversion method does not require discretization and can be performed in a single timestep over the whole time interval $[0, T]$.

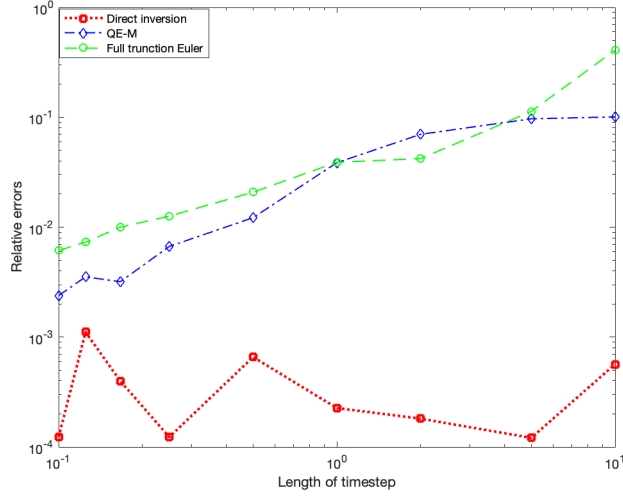


Figure 2: We show the relationship between the relative errors and the length of the timesteps in each simulation path for the full truncation Euler method, the QE-M method, and the direct inversion method. The number of simulation paths is 10^6 .

Table 2: We show the maximum length of timesteps in each simulation path and the CPU times to price the put option with approximation accuracy $O(10^{-3})$ for the full truncation Euler method, the QE-M method, and the direct inversion method. We simulate 10^6 paths in each case.

	Full Truncation Euler	QE-M	Direct-Inversion
Relative Error	6.14×10^{-3}	3.85×10^{-3}	3.12×10^{-3}
Length of timestep h	1/10	1/4	10
CPU time	28.38	6.14	0.42

Remark 2. As shown in Figure 2, when we simulate with 10^6 paths, the relative errors of the estimated option price by our direct inversion method is of order 10^{-3} , which is essentially caused by the Monte Carlo error. The data for the direct inversion method in Table 2 and Figure 2 is generated by the Chebyshev expansion with accuracy $O(10^{-4})$. In Figure 3, we show the relative errors and the CPU times of the direct inversion method using the two-dimensional Chebyshev expansion with accuracy $O(10^{-4})$ and with accuracy $O(10^{-8})$. The first three data points (from left to right) are generated with 10^4 , 10^5 , and 10^6 number of paths, which lead to Monte Carlo errors of order 10^{-2} , $10^{-2.5}$, and 10^{-3} . In these cases, the Chebyshev approximations with accuracy $O(10^{-4})$ and with accuracy $O(10^{-8})$ have comparable relative errors, whereas the Chebyshev approximation with accuracy $O(10^{-8})$ requires more CPU time. Since in these cases the Monte Carlo errors dominates the relative errors, the higher-accuracy Chebyshev expansion will not have a significant effect on the relative errors. Therefore, in these situations we can reduce the accuracy of the Chebyshev expansion to the same order as the Monte Carlo errors resulting in less CPU time while retaining the approximation accuracy. The last two data points

(from left to right) are generated with 10^7 and 10^8 number of paths, which lead to Monte Carlo errors of order $10^{-3.5}$ and 10^{-4} , respectively. For the Chebyshev approximation with accuracy $O(10^{-4})$, the relative errors remain at level $O(10^{-3})$ while for the Chebyshev approximation with error $O(10^{-8})$, the relative errors decrease further to about $O(10^{-4})$. Hence to achieve an efficient approximation, the accuracy of the Chebyshev approximation should be chosen to match the relative Monte Carlo error.

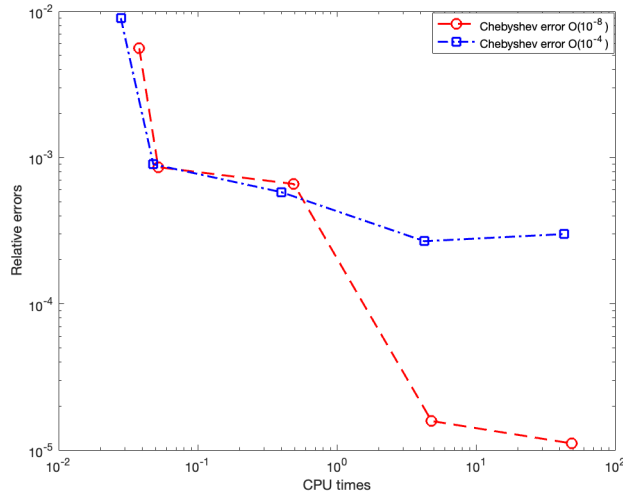


Figure 3: We compare the relative errors and CPU times of the direct inversion method using the two-dimensional Chebyshev expansion with accuracy $O(10^{-4})$ and $O(10^{-8})$. The number of paths in each simulation is $[10^4, 10^5, 10^6, 10^7, 10^8]$ (from left to right) which lead to Monte Carlo errors of order $[10^{-2}, 10^{-2.5}, 10^{-3}, 10^{-3.5}, 10^{-4}]$.

4.2 Path-dependent options: an Asian option

We apply our direct inversion method to the pricing of a path-dependent option. Here we consider an Asian option with a payoff function as follows:

$$\max \left(K - \frac{1}{M} \sum_{m=1}^M X_{t_m}, 0 \right),$$

where K is the strike price, and X_{t_m} is the asset price at the monitor times $0 = t_0, t_1, \dots, t_M = T$, and $t_m = mT/M$. As above, to simulate the CIR process X we use our direct inversion method to simulate the squared Bessel process first, and then use the simulated squared Bessel process to generate the CIR process as described in equation (2).

We apply the full truncation Euler method, the QE-M method, and the direct inversion method

to the pricing of the Asian option with yearly fixings and with quarterly fixings. The parameter values are same as for the put option in Section 4.1. For both cases of yearly fixings and quarterly fixings, the direct inversion method achieves high accuracy with a standard deviation of order 10^{-5} . The CPU time required compares favourably with the CPU times of the full truncation Euler method and of the QE-M method for the same level of accuracy (shown in the last line for each case in Table 3). Similar to the case of the put option considered above, the reason for this is that the direct inversion method does not require any discretization other than at the monitoring times, while the full truncation Euler method and the QE-M method require a finer sampling rate. For the direct inversion method the monitoring frequency in a path-dependent option determines the times at which the path must be simulated. Thus the required monitoring frequency may have an effect on the efficiency of the direct inversion method.

Table 3: We present the estimation results of the full truncation Euler method, the QE-M method and our direct inversion method using 10^6 paths for an Asian option with yearly fixings and quarterly fixings. In each case the triple shown is the estimated price, the sample standard deviation (inflated by 10^3) and CPU time. We test the full truncation Euler methods and the QE-M method with different lengths of timestep h . However, for the direct inversion method, the length of the timestep does not influence the approximation accuracy.

Stepsize	Full Truncation Euler	QE-M	Direct inversion
M=10			
h=1	[0.0366, 0.0473, 6.98]	[0.0469, 0.0358, 1.12]	[0.0464, 0.0341, 4.49]
h=1/2	[0.0416, 0.0349, 13.29]	[0.0463, 0.0347, 2.58]	
h=1/4	[0.0445, 0.0343, 26.12]	[0.0464, 0.0341, 6.88]	
M=40			
h=1/4	[0.0416, 0.0331, 25.89]	[0.0446, 0.0328, 6.28]	[0.0444, 0.0323, 17.89]
h=1/8	[0.0432, 0.0326, 51.22]	[0.0445, 0.0325, 15.89]	
h=1/16	[0.0446, 0.0325, 104.62]	[0.0444, 0.0323, 36.28]	

4.3 Basket option

We consider a basket option with payoff function

$$\max \left(K - \sum_{i=1}^d w_i X^{(i)}, 0 \right),$$

where d is the number of assets underlying the basket option, w_i is the weight of each asset, and the underlying asset $X^{(i)}$ is given as a CIR process

$$dX_t^{(i)} = (a_i + b_i X_t^{(i)}) dt + c_i \sqrt{X_t^{(i)}} dW_t^{(i)},$$

with constants a_i, b_i, c_i for $i = 1, \dots, d$.

Recall X can be expressed as a scaled and time-changed Bessel process $X_T^{(i)} = e^{b_i T} Y_{C(T)}^{(i)}$, where $Y^{(i)}$ is a squared Bessel process, and where the function C is given in equation (1). We have

$Y_{C(T)}^{(i)} = (C(T) - C(0)) \cdot \chi_{\delta_i}^2(\lambda_i)$ with $\delta_i = 4a_i/c_i^2$ and $\lambda_i = Y_{C(0)}^{(i)} / (C(T) - C(0))$. We use our direct inversion method to price the basket option for different parameter values a_i , b_i , and c_i . The values for a_i , b_i , and c_i are shown in Table 4. We consider different values of δ_i , b_i , and c_i . Since $a_i = \delta_i \cdot c_i^2/4$, here the parameter a_i is treated as a fixed parameter that depends on the values of δ_i and c_i . We set $T = 10$, $K = 0.09$, $d = 5$, $X_0^{(i)} = 0.09$, $Y_{C(0)}^{(i)} = 0.09$, and $w_i = 1/5$ for $i = 1, \dots, 5$.

To simulate the CIR process, we need to generate the non-central chi-square samples $\chi_{\delta_i}^2(\lambda_i)$. Recall we have $\chi_{\delta_i}^2(\lambda_i) = \chi_{\delta_i}^2 + \chi_{2N_i}^2$ where N_i is a Poisson random variable with mean $\lambda_i/2$. The first central chi-square sample $\chi_{\delta_i}^2$ is generated by our direct inversion method using common random numbers for all assets in the basket option, i.e., we generate $\chi_{\delta_1}^2, \dots, \chi_{\delta_5}^2$ from the same Uniform[0, 1] random variables. The second central-chi square sample $\chi_{2N_i}^2$ is generated with the method introduced in Malham and Wiese [15] and described in Section 3.2. For assets $X^{(i)}$ with parameter combinations (a_i, c_i) that result in the same degrees of freedom $\delta = \delta_i = 4a_i/c_i^2$, we only need to generate one central chi-square variable χ_{δ}^2 that can be used for all of these assets. For example, in cases 1 and 2, we have a fixed value of the degrees of freedom $\delta_i \equiv 0.18$, which means we generate one central chi-square sample $\chi_{\delta_i}^2$ only and use it in the simulation of all five assets in the basket option. In cases 3 and 4, the value of the degrees of freedom δ_i for each asset is different. Hence, we generate new central chi-square samples $\chi_{\delta_i}^2$ for each asset, resulting in longer CPU times as shown in Table 4. The CPU times in cases 1 and 2 are nearly the same, whereas the value of parameter b_i varies. This indicates our method is robust and not affected by the choice of value for the parameter b_i . By comparing cases 3 and 4, we also see that the change in value of parameter c_i does not affect the efficiency of our direct inversion method.

For comparison with our direct inversion method we choose the most favourable case for the full truncation Euler method of using the same driving Brownian motion for all five assets underlying the basket option. We choose the discretization timestep $h = 1/10$ for the full truncation Euler method to simulate the assets $X_{t_1}^{(i)}, \dots, X_{T_N}^{(i)}$ with $N = T/h$ to achieve an approximation accuracy comparable with our direct inversion method. The prices of the basket options are slightly different when using the full truncation Euler method compared with the direct inversion method. This is because the same seeds are used to generate the random variables driving the asset price processes in the full truncation Euler method. For the direct inversion method, only the first central chi-square sample $\chi_{\delta_i}^2$ are generated by the same seeds; the second central chi-square sample $\chi_{2N_i}^2$ cannot be generated with the same seeds because different values of parameters will lead to different means of the Poisson variables N_i . The CPU times in the five cases are nearly identical for the full truncation Euler method. Because the asset processes have different parameter values, every asset path needs to be generated by the full truncation Euler method (although with the same seed). In all five cases, our direct inversion method compares favourably in the CPU times, especially for case 1 and 2 with fixed degrees of freedom δ_i .

Table 4: We present the estimation results of the full truncation Euler method and the direct inversion method using 10^6 paths for a basket option with five assets. In each case the triple shown is the estimated price, the sample standard deviation (inflated by 10^3) and CPU times.

Case 1	
Degree of freedom δ	$\delta_i = 0.18$, for $i = 1, \dots, 5$
Free parameters	$b_i = -0.5$, for $i = 1, \dots, 5$ $[c_1, c_2, c_3, c_4, c_5] = [0.8, 0.9, 1, 1.1, 1.2]$
Fixed parameter	$[a_1, a_2, a_3, a_4, a_5] = [0.0288, 0.0365, 0.0450, 0.0545, 0.0648]$
Full truncation Euler method	[0.0666, 0.0350, 10.46]
Direct inversion method	[0.0690, 0.0344, 1.81]
Case 2	
Degree of freedom δ	$\delta_i = 0.18$, for $i = 1, \dots, 5$
Free parameters	$[b_1, b_2, b_3, b_4, b_5] = [-0.4, -0.45, -0.5, -0.55, -0.6]$ $[c_1, c_2, c_3, c_4, c_5] = [0.8, 0.9, 1, 1.1, 1.2]$
Fixed parameter	$[a_1, a_2, a_3, a_4, a_5] = [0.0288, 0.0365, 0.0450, 0.0545, 0.0648]$
Full truncation Euler method	[0.0666, 0.0349, 10.39]
Direct inversion method	[0.0692, 0.0344, 1.90]
Case 3	
Degree of freedom δ	$[\delta_1, \delta_2, \delta_3, \delta_4, \delta_5] = [0.1152, 0.1458, 0.1800, 0.2178, 0.2592]$
Free parameters	$b_i = -0.5$, $c_i = 1$, for $i = 1, \dots, 5$
Fixed parameter	$[a_1, a_2, a_3, a_4, a_5] = [0.0288, 0.0365, 0.0450, 0.0545, 0.0648]$
Full truncation Euler method	[0.0642, 0.0354, 10.65]
Direct inversion method	[0.0676, 0.0346, 2.59]
Case 4	
Degree of freedom δ	$[\delta_1, \delta_2, \delta_3, \delta_4, \delta_5] = [0.2250, 0.2000, 0.1800, 0.1636, 0.1500]$
Free parameters	$b_i = -0.5$, for $i = 1, \dots, 5$ $[c_1, c_2, c_3, c_4, c_5] = [0.8, 0.9, 1, 1.1, 1.2]$
Fixed parameter	$a_i = 0.045$, for $i = 1, \dots, 5$
Full truncation Euler method	[0.0649, 0.0350, 10.76]
Direct inversion method	[0.0679, 0.0344, 2.69]

5 Conclusion

In this paper, we designed a new direct inversion method to generate non-central chi-square samples and hence to simulate the squared Bessel process. The method is based on a two-dimensional Chebyshev approximation of the inverse distribution function, where the degrees of freedom of the chi-square sample are treated as one of the variables. Hence we can use the same series of Chebyshev coefficients to generate chi-square samples for a range of values for the degrees of freedom, making our method particularly efficient in such a setting. The direct inversion method is efficient and of high accuracy in generating chi-square samples for all degrees of freedom, particularly for the case of small degrees of freedom. High accuracy here means using

a Chebyshev expansion with accuracy of order 10^{-8} . In principle, our method can be extended to a higher order, such as the order 10^{-10} accuracy Chebyshev expansion in Malham and Wiese [15]. As a direct inversion method, the accuracy of the method does not depend on the length of the timestep in path simulations of the squared Bessel process, an important factor for the efficiency of the method.

We list some directions for future research. Firstly, since we have treated the degrees of freedom δ , or equivalently the dimension of the squared Bessel process, as a variable in our Chebyshev expansion, we can analyse the impact the model parameter δ has on the model and on the method. Secondly, we can use the simulated squared Bessel process to simulate other stochastic models, such as the CEV model. We can extend our two-dimensional Chebyshev expansion to the simulation of the Heston model, see also Malham, Shen, and Wiese [14] who established direct inversion algorithms for this model. Also see Malham and Wiese [16]. In particular, it will be interesting to explore our method for the calibration of the CIR process and of the Heston model, see also Cui, Rollin, and Germano [5] for a calibration algorithm based on the Heston characteristic function. Thirdly, we can consider extending our direct inversion method from the one-dimensional squared Bessel process to its matrix-valued extension, the Wishart process.

A Appendix

Table 5: The Chebyshev coefficients for the first region with $u \in [0, 0.1]$ and $\delta \in [0.1, 0.2]$ to achieve $O(10^{-8})$ approximation accuracy.

	0	1	2
0	0.0015173224201204	0.0002528722215717	-0.0000114009960766
1	0.0028185551650815	0.0004053700919312	-0.0000259448708964
2	0.0022599358279589	0.0001678268383677	-0.0000289961611465
3	0.0015680342698270	-0.0000700741494637	-0.0000215492684447
4	0.0009459043966500	-0.0002038468732949	-0.0000031908343145
5	0.0005000148204097	-0.0002183501508953	0.0000155516275132
6	0.0002342786936571	-0.0001632918130127	0.0000245736522666
7	0.0000986660876581	-0.0000957800587457	0.0000226176037315
8	0.0000378469221872	-0.0000462238395762	0.0000151912638058
9	0.0000133301455983	-0.0000188923951304	0.0000079916328208
10	0.0000043196173257	-0.0000067083849095	0.0000034157501336
11	0.0000012906319703	-0.0000020933533018	0.0000012177333308
12	0.0000003609030015	-0.0000005962987155	0.0000003726832304
13	0.0000000998616155	-0.0000001639159899	0.0000001012588862
	3	4	5
0	0.0000009598467591	-0.0000001024227037	0.0000000122727754
1	0.0000020896532161	-0.0000002151292692	0.0000000253707092
2	0.0000026001630603	-0.0000002531116714	0.0000000283544586
3	0.0000030696202825	-0.0000003242049038	0.0000000349527349
4	0.0000025977096176	-0.0000003843685990	0.0000000452799900
5	0.0000007618438592	-0.0000003286102337	0.0000000524580734
6	-0.0000015917811532	-0.0000000962454381	0.0000000424043844
7	-0.0000030850135229	0.0000002177742833	0.0000000100802685
8	-0.0000031377435380	0.0000004295129270	-0.0000000360000115
9	-0.0000022459349254	0.0000004469913959	-0.0000000647989030
10	-0.0000012247484604	0.0000003229989112	-0.0000000647743390
11	-0.0000005277189063	0.0000001662032187	-0.0000000454779202
12	-0.0000001871835099	0.0000000742134452	-0.0000000243260099
13	-0.0000000544287724	0.0000000250134666	-0.0000000097375780

Table 6: The Chebyshev coefficients for the middle region with $u \in [0.1, 1]$ and $\delta \in [0.1, 0.2]$ to achieve $O(10^{-8})$ approximation accuracy.

	0	1	2	3
0	0.3875945631074440	0.0026135656106857	0.0000129352935356	-0.0000000381872506
1	0.4956109866348150	0.0008953566937339	-0.0000067054601666	-0.0000000125588670
2	0.1197964723594020	-0.0027935601066155	-0.0000166388049599	0.0000000730650209
3	-0.0010763253182188	-0.0009194311880306	0.0000085829238628	0.0000001335013439
4	-0.0023865415596642	0.0001990751020187	0.0000035794963500	-0.0000000521728813
5	0.0004865330909205	0.0000201874711514	-0.0000020552522115	-0.0000000169016304
6	-0.0000106448822976	-0.0000192517056677	0.0000002053193871	0.0000000182461114
7	-0.0000205224390034	0.0000042306504504	0.0000001643278424	-0.0000000050681230
8	0.0000062842657989	0.0000000655856784	-0.0000000840329782	-0.0000000005964520
9	-0.0000007508885322	-0.0000003315298971	0.0000000156952882	0.0000000010012989
10	-0.0000001157724046	0.0000001086938654	0.0000000020326053	-0.0000000003785164
11	0.0000000777284278	-0.0000000140930457	-0.0000000022683390	0.0000000000505659

Table 7: The Chebyshev coefficients for the tail region with $u \in [1, \infty]$ and $\delta \in [0.1, 0.2]$ to achieve $O(10^{-8})$ approximation accuracy.

	0	1	2	3
0	6.8753214515317200	0.0154069212636548	-0.0000209599465735	-0.0000000864515313
1	8.5433821730433800	0.0090024260671873	-0.0000377801621097	-0.0000000303548005
2	3.4476658871478400	-0.0130690823892008	0.0000022840388153	0.0000000362919660
3	0.9330390647038300	-0.0087472864187297	0.0000347919528143	0.0000000562970750
4	0.1741822695325730	-0.0023271850423403	0.0000189337983037	-0.0000000495179004
5	0.0231441815282366	-0.0002445078701620	0.0000029857164456	-0.0000000266197129
6	0.0027835177479455	-0.0000075113568411	-0.0000003271927323	0.0000000028475004
7	0.0004380896611385	-0.0000109856591271	0.0000000145476511	0.0000000029205683
8	0.0000474342757583	-0.0000033230341686	0.0000000850337842	-0.0000000002011847
9	-0.0000039453038556	0.0000003821206797	-0.0000000061400030	-0.0000000040928856
10	-0.0000006163799253	0.0000001912780830	-0.0000000172232771	0.0000000086484494
11	0.0000004418045229	-0.0000000406903687	-0.0000000104246286	0.0000000086001421
12	0.0000000377188891	-0.0000000175539467	-0.0000000096591111	0.0000000085524035
13	-0.0000000336347029	0.0000000003271218	-0.0000000102016363	0.0000000085537387

References

- [1] J. H. Ahrens and U. Dieter. Computer methods for sampling from gamma, beta, poisson and binomial distributions. *Computing*, 12(3):223–246, 1974.
- [2] L. Andersen. Simple and efficient simulation of the Heston stochastic volatility model. *Journal of Computational Finance*, 11(3):1–43, 2008.
- [3] N. Basu. On double Chebyshev series approximation. *SIAM Journal on Numerical Analysis*, 10(3):496–505, 1973.
- [4] J. C. Cox, J. E. Ingersoll Jr, and S. A. Ross. A theory of the term structure of interest rates. In *Theory of valuation*, pages 129–164. World Scientific, 2005.
- [5] Y. Cui, S. del Baño Rollin, and G. Germano. Full and fast calibration of the Heston stochastic volatility model. *European Journal of Operational Research*, 263(2):625–638, 2017.
- [6] M. Gaß, K. Glau, M. Mahlstedt, and M. Mair. Chebyshev interpolation for parametric option pricing. *Finance and Stochastics*, 22:701–731, 2018.
- [7] P. Glasserman. *Monte Carlo Methods in Financial Engineering*. Springer-Verlag, 2004.
- [8] P. Glasserman and K.-K. Kim. Gamma expansion of the Heston stochastic volatility model. *Finance and Stochastics*, 15:267–296, 2011.
- [9] A. Göing-Jaeschke and M. Yor. A survey and some generalizations of Bessel processes. *Bernoulli*, 9(2):313–349, 2003.
- [10] B. Hu, D. A. Kessler, W.-J. Rappel, and H. Levine. How input fluctuations reshape the dynamics of a biological switching system. *Physical Review E*, 86(6):061910, 2012.
- [11] M. Jeanblanc, M. Yor, and M. Chesney. *Mathematical Methods for Financial Markets*. Springer Science & Business Media, 2009.
- [12] N. Johnson. On an extension of the connexion between Poisson and χ^2 distributions. *Biometrika*, 46(3/4):352–363, 1959.
- [13] R. Lord, R. Koekkoek, and D. V. Dijk. A comparison of biased simulation schemes for stochastic volatility models. *Quantitative Finance*, 10(2):177–194, 2010.
- [14] S. J. A. Malham, J. Shen, and A. Wiese. Series expansions and direct inversion for the Heston model. *SIAM Journal on Financial Mathematics*, 12(1):487–549, 2021.
- [15] S. J. A. Malham and A. Wiese. Chi-square simulation of the CIR process and the Heston model. *International Journal of Theoretical and Applied Finance*, 16(03):1350014, 2013.
- [16] S. J. A. Malham and A. Wiese. Efficient almost-exact Lévy area sampling. *Statist. Probab. Lett.*, 88:50–55, 2014.
- [17] G. Marsaglia and W. W. Tsang. A simple method for generating Gamma variables. *ACM Transactions on Mathematical Software (TOMS)*, 26(3):363–372, 2000.

- [18] B. Moro. The full Monte. *Risk*, 8(2):57–58, 1995.
- [19] J. Pitman and M. Winkel. Squared Bessel processes of positive and negative dimension embedded in Brownian local times. *Electronic Communications in Probability*, 23:1 – 13, 2018.
- [20] J. Pitman and M. Yor. A decomposition of Bessel bridges. *Zeitschrift für Wahrscheinlichkeitstheorie und verwandte Gebiete*, 59(4):425–457, 1982.
- [21] J. Pitman and M. Yor. Infinitely divisible laws associated with hyperbolic functions. *Canadian Journal of Mathematics*, 55(2):292–330, 2003.
- [22] W. H. Press, W. T. Vetterling, S. A. Teukolsky, and B. P. Flannery. *Numerical recipes in C++ the art of scientific computing*. Cambridge University Press, 2001.
- [23] D. Revuz and M. Yor. *Continuous Martingales and Brownian Motion*, volume 293. Springer Science & Business Media, 2013.
- [24] E. Scheiber. On the Chebyshev approximation of a function with two variables. *Bulletin of the Transilvania University of Brasov, Series III: Mathematics, Informatics, Physics*, 8, 2015.
- [25] A. F. Siegel. The noncentral chi-squared distribution with zero degrees of freedom and testing for uniformity. *Biometrika*, 66(2):381–386, 1979.
- [26] L. N. Trefethen. *Approximation Theory and Approximation Practice, Extended Edition*. SIAM, 2019.
- [27] D. Vere-Jones and T. Ozaki. Some examples of statistical estimation applied to earthquake data: I. cyclic poisson and self-exciting models. *Annals of the Institute of Statistical Mathematics*, 34:189–207, 1982.